To cite this article: MAO L W, ZHU X M, HUANG Z X, et al. Impact response of composite lattice sandwich plate structure subjected to underwater explosion[J/OL]. Chinese Journal of Ship Research, 2022, 17(3). http://www.ship-research.com/en/article/doi/10.19693/j.issn.1673-3185.02503.

DOI: 10.19693/j.issn.1673-3185. 02503

Shock response of composite lattice sandwich structure subjected to underwater explosion

MAO Liuwei[1], *ZHU Xinming*[2], *HUANG Zhixin*[3], *LI Ying*[*3]

1 Naval Research Academy, Beijing 100161, China

2 School of Science, Wuhan University of Technology, Wuhan 430063, China

3 Institute of Advanced Structure Technology, Beijing Institute of Technology, Beijing 100081, China

Abstract: [**Objective**] In order to improve the anti-explosion performance of ships subjected to the underwater explosion, this paper studies the anti-shock performance and energy absorption of the new protective structure consisting of carbon fiber reinforced plastic (CFRP) and lattice aluminum sandwich plate. [**Methods**] First, finite element software ABAQUS is used to establish the numerical simulation model of the CFRP-lattice aluminum sandwich plate under nonexplosive and noncontact underwater explosion load, and its reliability is verified. Single variables are then controlled to analyze the influence of the fiber layer thickness of the upper and lower panels and the rod diameter of the lattice sandwich structure on the energy absorption performance and structural deflection of the CFRP-lattice aluminum sandwich plate. Finally, based on the above three design parameters, surrogate optimization models are established by using experimental design and numerical simulation methods to optimize the energy absorption of the CFRP-lattice aluminum sandwich plate. [**Results**] The results show that when the mass of the CFRP-lattice aluminum sandwich plate is constant, the specific energy absorption (*SEA*) of the optimized results can be increased by 284%. In full consideration of the deformation of the lower panel, the *SEA* of the optimized results can be increased by 59%. [**Conclusions**] This paper shows that the proposed optimized structure of CFRP-lattice aluminum sandwich plate can effectively improve their energy absorption performance, and the response surface methodology (RSM) is an optimization method that can effectively strengthen the energy absorption performance of the structure.

Key words: underwater explosion; lattice structure; optimization design; numerical simulation

CLC number: U661.4

0 Introduction

Underwater explosion is one of the main loads damaging ships, and it will seriously threaten the vitality of ships. Underwater explosion can be divided into three important stages: explosive detonation, shock wave propagation, and bubble pulsation [1-3]. Ref. [4] described in detail the physical and chemical phenomena and their changes at different stages of underwater explosion, analyzed the distribution and propagation characteristics of underwater explosion load, and established the classical semi-empirical and semi-theoretical formula for the underwater explosion shock wave load. The theory is still in use and has been continuously developed and perfected. A large number of scholars have studied the underwater explosion phenomenon and the shock wave load characteristics. Geers [5] proposed the doubly asymptotic approximation (DAA) method, which is a method for solving the fluid-solid coupling load in advance. The method is also known as a decoupling method and has been continuously de-

Received: 2021 − 08 − 26 **Accepted**: 2022 − 06 − 20

Supported by: The National Natural Science Foundation of China (11802030)

Authors: MAO Liuwei , male, born in 1985, PhD, senior engineer. Research interests: explosion damage assessment on ships and overall demonstration research on ships. E-mail: mlw_18@163.com

LI Ying, male, born in 1988, PhD, professor. Research interests: explosion damage and protection. E-mail: bitliying@bit.edu.cn

***Corresponding author**: LI Ying

veloped and improved during its application in the underwater explosion. Li et al. [6] obtained the corresponding shock spectrum by measuring the dynamic response of the floating shock platform under the underwater explosion load. It was found that the three stages in the shock spectrum corresponded to the shock wave generated by the underwater explosion, the after flow induced by the bubble motion, and the bubble pulsating pressure, respectively. Xin et al. [2] compared the performance of different numerical simulation software under the action of underwater explosion load and found that ABAQUS had great advantages in calculating far-field explosion, with a fast calculation speed and good stability. Zhang et al. [1] reviewed and analyzed the current research status of the underwater explosion in terms of the real ship experiment, theoretical analysis, and numerical method, and they summarized the characteristics of underwater explosion load and characteristics of its damage to ships.

To improve the vitality of ships, in recent years, scholars have carried out a large number of studies on the energy absorption performance of typical protective structures under explosion and shock loads, such as the honeycomb structure, foam structure, and lattice structure [7-16]. It is found that honeycomb and foam structures have high energy absorption efficiency, but their structural designability is low, and the anti-shock performance is difficult to be improved. Metal porous lattice structure has high designability, three-dimensional periodicity, low apparent density, and large porosity, and thus it can effectively absorb the energy of shock load. With the rapid development of additive manufacturing (AM) technology, the lattice structure has been widely used in fields such as ships, aerospace, and automobile. Ostos et al. [7] divided the compressive stress – strain curve of the lattice structure into three stages, namely, the linear elastic stage, plateau stage, and densification stage. Elsayyed et al. [17] proposed an octet-truss lattice structure. Ushijima et al. [18] theoretically calculated the mechanical properties of the single cells of the body-centered cubic (BCC) cell and found that a decrease in the aspect ratio of single cells and an increase in the diameter of pillars can help to improve the initial stiffness and plastic failure strength of single cells.

In addition to porous materials, fiber reinforced plastic (FRP) is widely used in the anti-shock field due to its high specific stiffness and specific strength [19]. Since the brittleness of fiber is destroyed under a shock load, its energy absorption efficiency is relatively low. But the combination of FRP and metal porous lattice structure can achieve better anti-shock performance as it considers both the ductility of the metal and the high specific strength of composite materials. However, the damage and energy dissipation mechanisms of the composite material-lattice sandwich structure subjected to underwater explosion load are still unclear.

In this paper, a carbon fiber reinforced plastic (CFRP) plate and a lattice aluminum sandwich structure are combined to form a new composite material-lattice sandwich plate structure, and its anti-explosion and anti-shock performance under underwater explosion shock wave load will be studied. At the same time, the dynamic response is quantified as a function design relationship among the geometric parameters of the sandwich plate, and the optimal structural design parameters are found to maximize the energy absorption, so as to provide the reference for studying the shock response of the composite sandwich plate structure under noncontact underwater explosion shock wave load. Firstly, the dynamic response of the CFRP-lattice aluminum sandwich plate with different structural parameters subjected to noncontact underwater explosion shock wave load is numerically simulated by the finite element software ABAQUS. Then, the energy absorption and deformation of the CFRP-lattice aluminum sandwich plate structure are optimized to improve the protective performance of the structure.

1 Materials and methods

1.1 Response surface methodology (RSM) and its theory

The anti-shock problem of the sandwich plate structure subjected to underwater explosion shock wave load features large geometric deformation and high nonlinearity. Traditional optimization methods have great limitations, so the surrogate method is generally used for solutions. The surrogate optimization method is essentially an approximate alternative method, and it involves RSM, Kriging method, radial basis neural network method, artificial neural network method, etc. These methods establish surrogate optimization models by fitting or interpolation and estimate the response information of unknown points by the response information of known points. Among them, RSM is one of the most effective alternative methods to solve related problems, and it

is a commonly used method in solving multivariable issues and analyzing system reliability. Furthermore, it is widely applied in various engineering fields such as structural crashworthiness, tube hydroforming, laser cutting, and welding process [20-21].

RSM, namely, the response surface design method, is a design of experiment (DOE) technique that helps to understand and optimize the response. If certain factors are believed or suspected to have nonlinear effects on the objective, a mathematical function containing the first and square terms of these main factors can be established to predict the relationship between the target response value and these factors, and the optimal experimental conditions for multidisciplinary design optimization problems can be obtained accurately and efficiently with short experimental cycles and few experiments. For response surface optimization, an appropriate basis function form shall be firstly selected to establish the undetermined relationship between the design variables and the output of the results. Then, the DOE method is used to collect samples in the design domain, and numerical analysis of the sample points is carried out. In addition, the basis function is fitted by the least square method. Finally, the approximate surrogate optimization problem is constructed and solved [21].

The response approximation function can be assumed as the sum of a set of basis functions.

$$f(x)=\sum_{i=1}^{L}a_i\phi_i(x) \tag{1}$$

where L is the number of the basis function ϕ_i; a_i is the undetermined constant; x is the design variable. The undetermined constant $\boldsymbol{a}=[a_1, a_2,\cdots, a_L]^{\mathrm{T}}$ is determined according to the minimum sum of squared errors between the actual response value and the approximation function.

$$\sum_{p=1}^{P}\left\{[y(x_p)-f(x_p)]^2\right\}=\sum_{p=1}^{P}\left\{\left[y(x_p)-\sum_{i=1}^{L}a_i\phi_i(x_p)\right]^2\right\} \tag{2}$$

where P is the number of experimental design points; $y(x_p)$ is the actual function response value at each point x_p, which constitutes $\boldsymbol{y}=[y_1, y_2,\ldots, y_p]^{\mathrm{T}}$.

The undetermined constant $\boldsymbol{a}$ is obtained as

$$\boldsymbol{a}=\left(\boldsymbol{X}^{\mathrm{T}}\boldsymbol{X}\right)^{-1}\boldsymbol{X}^{\mathrm{T}}\boldsymbol{y} \tag{3}$$

where $\boldsymbol{X}$ is the basis function matrix at each design point, and its form is as follows.

$$\boldsymbol{X}=\begin{bmatrix}\phi_1(x_1) & \cdots & \phi_L(x_1)\\ \vdots & \ddots & \vdots\\ \phi_1(x_p) & \cdots & \phi_L(x_p)\end{bmatrix} \tag{4}$$

There are a variety of forms of basis functions, and the commonly used ones include linear and quadratic complete polynomials.

$$\boldsymbol{\phi}=[1, x_1, x_2,\cdots, x_n]^{\mathrm{T}} \tag{5}$$

$$\boldsymbol{\phi}=\left[1, x_1,\cdots, x_n, x_1^2, x_1x_2,\cdots, x_1x_n,\cdots, x_n^2\right]^{\mathrm{T}} \tag{6}$$

The selection of sample points can be realized by using the orthogonal design method. The orthogonal design of linear regression can be conducted by using an orthogonal design table, and that of quadratic regression is usually carried out by central composite design (CCD) [21-22]. Fig. 1 shows one form of this method, and problems involving cubic polynomials or beyond are rare.

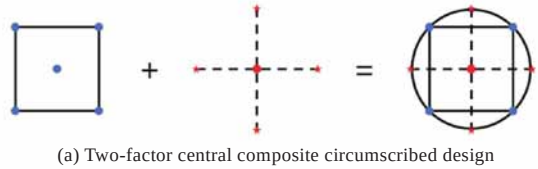

(a) Two-factor central composite circumscribed design

(b) Three-factor central composite circumscribed design

Fig. 1 Central composite circumscribed design

Another DOE method, namely, Latin hypercube sampling (LHS), was proposed by McKay et al. [23] in 1979. This method involves uniformly distributed sample points in space, and its process can be regarded as extracting m samples in an n-dimensional vector space. During the process, each dimension of the n-dimensional vector space is divided into m intervals of equal length, and one sample point from different intervals of each dimension is randomly selected. Then, a sample is formed by these randomly selected sample points. In total, m samples can be obtained. This is a very efficient method to ensure that all variable ranges are covered, as shown in Fig. 2.

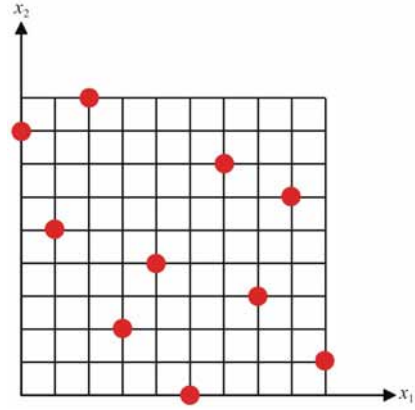

Fig. 2 Random LHS

1.2 Establishment of finite element model

To explore the dynamic response of the CFRP-lattice aluminum sandwich plate under nonexplosive and noncontact underwater explosion shock wave load, the finite element software ABAQUS was used to establish the calculation model. An explicit dynamic analysis was carried out by ABAQUS/Explicit, and a three-dimensional finite element simulation was carried out.

The whole finite element model consists of two CFRP panels and their sandwich layers, as well as a loading water tank. The length of the loading water tank is 600 mm, and the flying plate has a diameter and a thickness of 80 and 10 mm, respectively. The piston is 80 mm in diameter and 20 mm in thickness, and it goes deep into the shock tube and is flush with the tube mouth, with its spacing with the flying plate being 1 mm. The diameter and thickness of the upper and lower panels of the CFRP plate are 140 and 1 mm, respectively, and each panel has four fiber layers, with a thickness of 0.25 mm. The diameter of the effective area subjected to underwater shock wave load in the CFRP plate is 80 mm. There is only one sandwich layer, and its thickness is 5 mm. An aluminum lattice structure based on the Octet structure is used in the middle, which is composed of 16 × 16 cells. Each cell is built by the rod formed by 12 diagonal lines on the six outer surfaces of the cube and 12 lines connecting the center of adjacent surfaces inside the cube, and its length, width, and height are all 5 mm, with the diameter of the rod being 1 mm. The single cell structure is shown in Fig. 3(a). The sandwich plate structure is shown in Fig. 3(b), and the numerical simulation model is shown in Fig. 3(c). The flying plate, piston, loading water tank, and CFRP – lattice aluminum sandwich plate are modeled by the Lagrange method, and the water area is modeled by the Euler method.

1.3 Material constitutive model

The upper and lower panels of the CFRP plate are made from CFRP, which is formed by the infiltration and hardening of multilayer carbon fiber cloth through the epoxy resin. The carbon fiber cloth in this paper is made by a bidirectional weaving technology, or in other words, the fiber is bidirectionally distributed along the two vertical directions of the plane and woven by a certain technology. The planar stress – strain relationship in the fiber direction is orthogonal linear elasticity. The mechanical parameters of the CFRP plate are shown in Table 1.

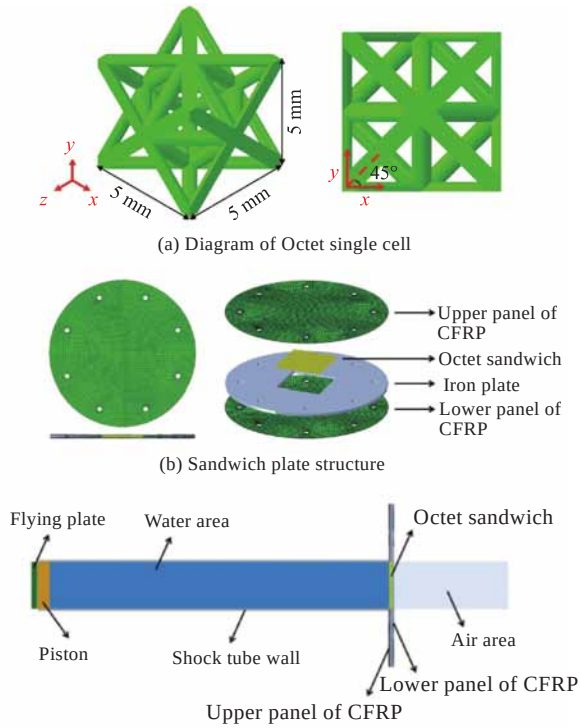

(a) Diagram of Octet single cell

(b) Sandwich plate structure

(c) Calculation model of shock response of CFRP-lattice aluminum sandwich plate

Fig. 3 Finite element model of CFRP-lattice aluminum sandwich plate

Table 1 Partial material parameters of CFRP plate (single layer)

Parameter	Value
Density /(g·cm^{-3})	1.56
Young's modulus /MPa	42 700
Shear modulus/MPa	4 400
Poisson's ratio	0.05
Tensile strength/MPa	658
Compressive strength/MPa	269
Initial shear stress of shear damage/MPa	37

The Octet lattice structure of the sandwich layer adopts aluminum alloy, and some material parameters are shown in Table 2 and Fig. 4.

The fluid medium in the shock tube is water, and

Table 2 Partial material parameters of aluminum alloy

Parameter	Value
Density /(g·cm^{-3})	2.7
Young's modulus/MPa	69 000
Poisson's ratio	0.33
Fracture strain	0.125

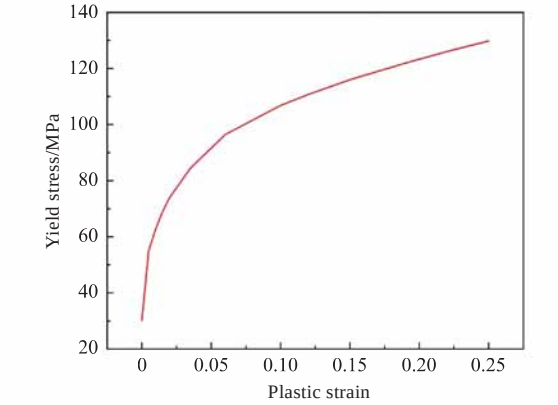

Fig. 4 Yield stress-plastic strain curve of aluminum alloy

the linear U_s-U_p Hugoniot state equation is used to simulate the viscous and nonviscous layered flow of an incompressible fluid. The specific form is

$$p = \frac{\rho_0 c_0^2 \eta}{(1-s\eta)^2}\left(1-\frac{\Gamma_0 \eta}{2}\right)+\Gamma_0 \rho_0 E_m \tag{7}$$

where p is the current pressure; ρ_0 is the initial density; c_0 is the sound velocity; η is the nominal volumetric compressive strain; Γ_0 is the material constant; E_m is the internal energy per unit mass; s is the Hugoniot slope coefficient. The relationship between the shock wave velocity U_s and the particle velocity U_p is as follows.

$$U_s = c_0 + sU_p \tag{8}$$

The parameters of water are shown in Table 3.

Table 3 Parameters of water

Parameter	Value
Density/(g·cm^{-3})	1
c_0/(m·s^{-1})	1 480
s	0
Γ_0	0
Specific heat/(J·kg^{-1}·℃$^{-1}$)	4.2×10^3
Dynamic viscosity/(Pa·s)	1×10^{-3}

1.4 Load, boundary conditions, and meshing

Deshpande et al. [24] carried out theoretical derivation for one-dimensional wave theory and considered that the peak pressure of the flow field at a distance could be adjusted by changing the initial velocity of the flying plate, and the decay rate of the shock wave could be adjusted by changing the mass of the flying plate and piston. It can be expressed as

$$p_0 = c_w \rho_w v_0 \tag{9}$$

$$\theta = \frac{m_p}{c_w \rho_w} \tag{10}$$

where p_0 is the peak pressure of the shock wave; c_w and ρ_w are the sound velocity in water and the density of water, respectively; v_0 is the initial velocity of the flying plate; m_p is the mass of the flying plate; θ is the decay time. In view of the sufficient reflection of the shock wave, the impulse I_0 acting on the stationary plate can be calculated through the following equation.

$$I_0 = 2\int_0^\infty p_0 e^{-\frac{t}{\theta}} dt = 2p_0\theta \tag{11}$$

According to the experimental principle of the nonexplosive underwater explosion shock wave loading system, the initial conditions of the system are set. The impact velocity of the flying plate is set as 10 m/s (it is an approximately far-field underwater explosion, and the peak value of the shock wave acting on the structure is about 15 MPa). The outer surface of the shock tube is fixed, and the CFRP-lattice aluminum sandwich plate is fixed by eight bolts. The total calculation time of the model is set to be 3 ms so that the lower panel of the CFRP plate can be rebounded, so as to meet the calculation requirements. The accuracy and efficiency of calculation should be considered in meshing. If the grid size is too large, the calculation accuracy of the software will be affected, which will make the calculated deflection (deformation) of the lower panel of the CFRP plate and the total energy of the model fail to meet the requirements. If the grid size is too small, the calculation efficiency of the software will be greatly reduced. Therefore, it is necessary to select an appropriate grid size. Before analyzing and discussing the grid size, the paper needs to verify the effectiveness of numerical simulation.

2 Results and discussion

2.1 Model verification

The calculation model of the solid plate made of 5A06 aluminum alloy under loading is established by ABAQUS, as shown in Fig. 5. Firstly, a noncontact underwater explosion simulation device [25-26] is used to impose a shock wave load on the aluminum plate. Then, the peak value of the shock wave measured by the pressure sensor at the loading position of the loading water tank is analyzed and compared with the experimental results of Huang et al. [27]. The whole finite element model consists of an aluminum plate and its sandwich layer, as well as a loading water tank. Specifically, the loading water tank has a length of 500 mm, and the pressure sensor is 20 mm away from the nozzle of the loading water tank. The diameter and mass of the flying

plate are 66 mm and 0.13 kg, respectively. The piston is 66 mm in diameter and 0.22 kg in mass. The piston goes into the shock tube and is flush with the tube mouth, and the spacing between the flying plate and the piston is 1 mm. The diameter and thickness of the aluminum plate are 160 and 0.5 mm, respectively. The diameter of the effective area subjected to underwater shock wave load in the aluminum plate is 66 mm. In the figure, the flying plate, piston, loading water tank, and aluminum plate are modeled by the Lagrange method, and the water area is modeled by the Euler method. The deflection of the aluminum plate perpendicular to the plane direction of the plate under underwater shock wave load is shown in Fig. 6, where U is the deflection of the aluminum plate, and U_3 is the deflection component perpendicular to the plane direction of the aluminum plate. Fig. 7 shows the peak pressure of the shock wave at the tube mouth. It can be seen that the difference in peak pressure between the numerical simulation method and the experiment is 10.5%, which verifies the effectiveness of the numerical method. At the same time, it can be considered that in a certain range, the influence of different Euler domain grid sizes on the dynamic response of the plate is slight. Therefore, in order to improve the calculation efficiency, the grid size of the Euler domain is defined as 5 mm.

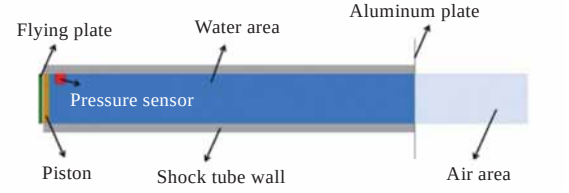

Fig. 5 Calculation model of shock response of aluminum plate

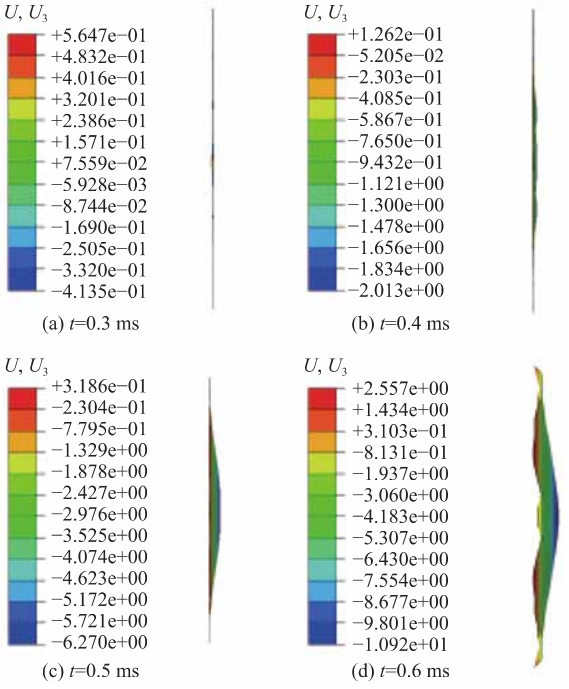

Fig. 6 Profile of deformation process of aluminum plate under underwater shock wave load

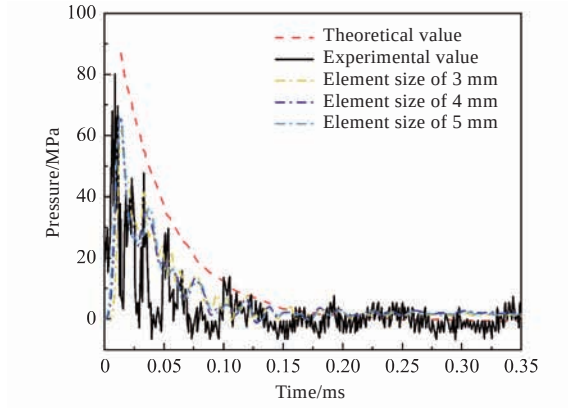

Fig. 7 Peak value of shock wave pressure at the tube opening

2.2 Dynamic response of CFRP-lattice aluminum sandwich plate under shock wave load

From the discussion in previous sections, the Euler domain grid size in the calculation model of the CFRP-lattice aluminum sandwich plate is set to 5 mm, and the grid size of the CFRP plate is set to 4 mm. The finite element simulation analysis of the dynamic response of the CFRP-lattice aluminum sandwich plate subjected to the nonexplosive and noncontact underwater explosion shock wave is carried out by ABAQUS. The model parameters are shown in Table 4.

Table 4 Model parameters of CFRP-lattice aluminum sandwich plate

Parameter	Value
Fiber layer thickness of upper panel t_1/mm	0.250
Rod diameter of Octet lattice t_2/mm	1.000
Fiber layer thickness of lower panel t_3/mm	0.250
Energy/J	107.211
Mass/kg	8.892
Specific energy absorption SEA/(J·kg^{-1})	12.057
Maximum deflection of the lower panel $Deflection$/mm	5.499

Through calculation, it is found that the deflection of the lower panel reaches the maximum at 1.77 ms. Then a rebound ensues, and the deflection begins to decrease. At this time, the Mises stress diagram of the upper and lower panels and the sandwich as well as the deflection diagram of the lower panel are shown in Fig. 8, where S is the Mises

stress, and U_4 is the deflection of the lower panel. It can be seen that the upper and lower panels and sandwich materials of the CFRP plate have not been damaged, and the maximum deformation occurs at the center of the lower panel of the CFRP plate. For the anti-explosion performance of the sandwich plate, the following parameters are used as indicators to evaluate the energy absorption effect, namely, the maximum deflection of the lower panel *Deflection* and the specific energy absorption *SEA*. The total energy absorbed by the structure is represented by E, and m is the total mass of the sandwich plate. *SEA* is used to measure the energy absorption performance per unit mass of the structure, which can be expressed as

$$SEA = \frac{E}{m} \tag{12}$$

The energy dissipation of CFRP is mainly manifested as matrix cracking, fiber fracture, and delamination, and the energy absorption of the sandwich exists as the plastic deformation of the lattice material, which accounts for the largest proportion of the total energy dissipation. In general, under the same conditions, the structure with thick panels can better absorb energy due to the use of more material. Therefore, the influence on the dynamic response will be explored by changing the fiber layer thickness of the upper and lower panels and the rod diameter of the Octet lattice sandwich structure.

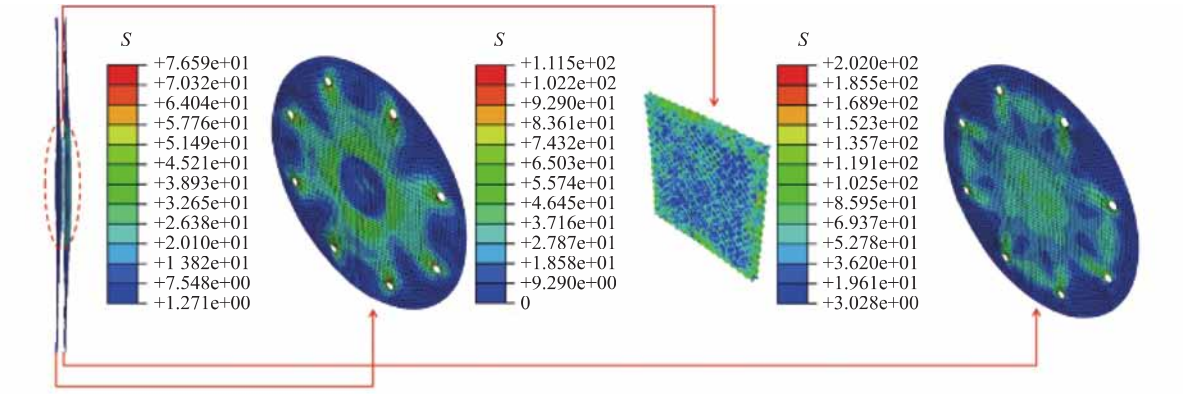

(a) Stress diagram of each part of CFRP-lattice aluminum sandwich plate

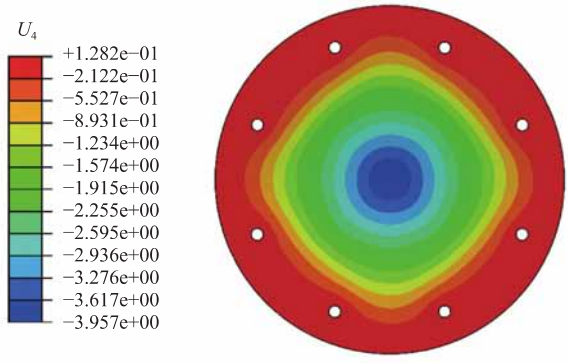

(b) Deflection diagram of lower panel of CFRP plate

Fig. 8 Dynamic response of CFRP plate

2.3 Influence of structural parameters on the dynamic response

2.3.1 Influence of fiber layer thickness of the upper panel

Since the manufacturing process of the carbon fiber composite plate will limit the thickness of panels. In theory, the thickness of a panel can only be controlled by changing the number of layers. In order to obtain the optimal solution by designing the function relationship, it is assumed that the thickness of the panel can change continuously. After determining the ideally optimal solution, this paper determines the optimal solution conforming to the process conditions according to the process requirements.

By keeping the rod diameter and lower panel thickness of the Octet lattice sandwich structure unchanged and changing the fiber layer thickness of the upper panel, the paper obtained the results is shown in Table 5 and Fig. 9. It can be seen that under the given three working conditions (working condition A, working condition B, and working condition C), as the fiber layer thickness of the upper

Table 5 Simulation results under different working conditions

Working condition	Fiber layer thickness of upper panel t_1/mm	Rod diameter of Octet lattice t_2/mm	Fiber layer thickness of lower panel t_3/mm	Energy/J	Mass/kg	*SEA*/(J·kg^{-1})	*Deflection*/mm
A	0.25	1.0	0.25	107.211	8.892	12.057	5.499
B	0.10	1.0	0.25	33.467	8.725	3.836	5.796
C	0.40	1.0	0.25	41.025	9.059	4.529	5.516
D	0.25	0.8	0.25	82.567	8.873	9.306	5.032
E	0.25	1.2	0.25	120.051	8.916	13.464	5.699
F	0.25	1.0	0.10	105.024	8.725	12.036	7.232
G	0.25	1.0	0.40	103.309	9.059	11.404	4.801

panel increases or decreases, *Deflection* does not change greatly, but it has a great influence on the energy absorption of the structure. At this time, compared with the gradient structure with only the thickness of the upper panel changed, the uniform structure has better energy absorption performance.

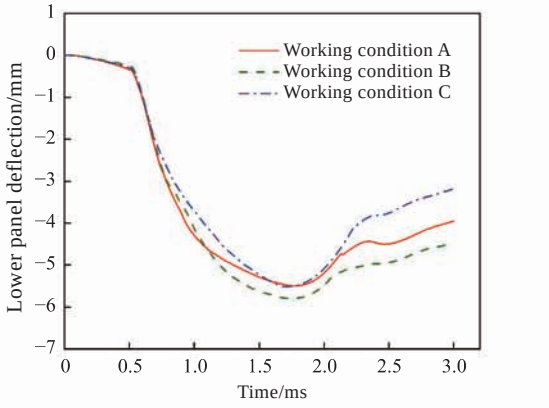

(a) Deflection-time curves of lwer panel

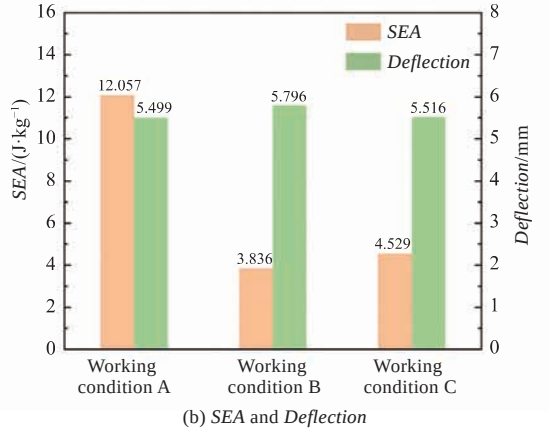

(b) *SEA* and *Deflection*

Fig. 9 Simulation results of changing the fiber thickness of each layer of the upper panel

2.3.2 Influence of rod diameter of lattice sandwich structure

By keeping the thickness of the upper and lower panels unchanged and changing the rod diameter of the Octet lattice sandwich structure, the paper obtained the results shown in Table 5 and Fig. 10. It can be seen that the Octet rod diameter has little effect on the deflection of the lower panel of the structure but has a great influence on the energy absorption performance of the structure under the three conditions (working condition A, working condition D, and working condition E). This can be explained by the fact that as the Octet rod diameter increases, the plastic deformation performance of the sandwich will greatly improve. As a result, more energy will be absorbed by the structure.

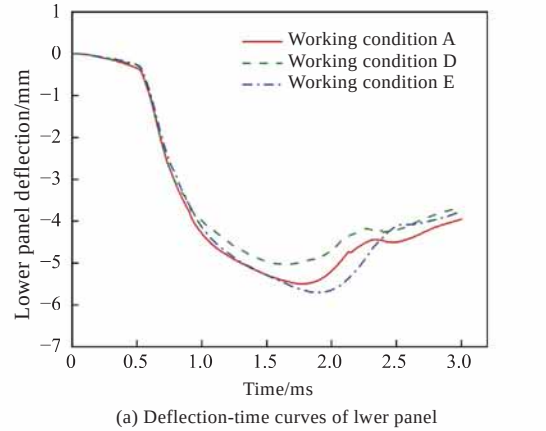

(a) Deflection-time curves of lwer panel

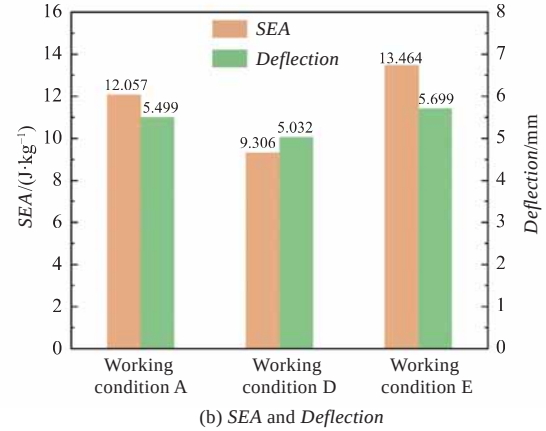

(b) *SEA* and *Deflection*

Fig. 10 Simulation results of changing the diameter of lattice rod

2.3.3 Influence of fiber layer thickness of the lower panel

By keeping the rod diameter of the Octet sandwich lattice structure and the thickness of the upper

panel unchanged and changing the thickness of the fiber layer thickness of the lower panel, the paper obtained the following results and showed them in Table 5 and Fig. 11. It can be seen that under the given three working conditions (working condition A, working condition F and working condition G), the thickness of the lower panel has a significant influence on the deflection of the lower panel of the structure but has a slight influence on the energy absorption of the structure. As the thickness of the lower panel improves, *Deflection* will get small, but the energy absorbed by the structure will decrease.

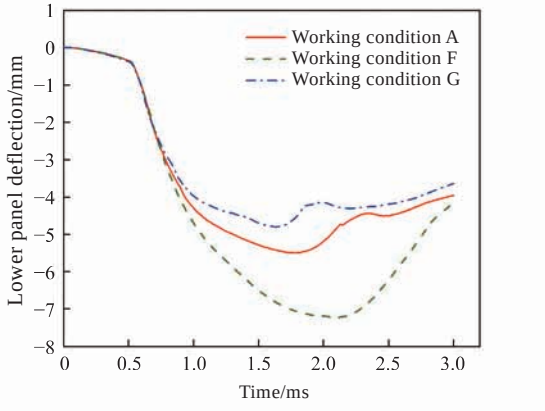

(a) Deflection-time curves of lwer panel

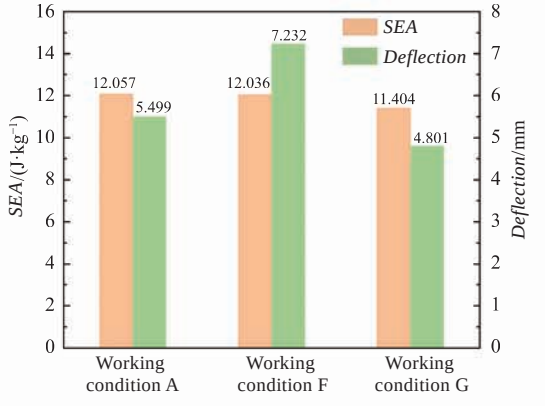

(b) *SEA* and *Deflection*

Fig. 11 Simulation results of changing the fiber thickness of each layer of the lower panel

In summary, the thickness of the upper and lower panels and the Octet rod diameter can affect the energy absorption performance and structural deflection of the CFRP-lattice aluminum sandwich plate. In order to further explore the change in the dynamic response of the model when the three structural parameters change at the same time and obtain the optimal design parameters, the paper must adopt the experimental design method.

2.4 Optimization design of CFRP-lattice aluminum sandwich plate

For the sandwich plate with equal mass, the existing research [28] shows that the gradient structure (i.e., the structure with uneven thickness) has better energy absorption performance than that of the uniform structure when the initial shock velocity is not very high. However, the influence of the thickness of the upper and lower panels and the Octet rod diameter on the energy absorption performance and structural deflection of the CFRP-lattice aluminum sandwich plate is interactive. To further explore the change in the dynamic response of the model when the three structural parameters change at the same time and obtain the optimal design parameters, this paper will use the RSM for the optimal design of the energy absorption of the CFRP-lattice aluminum sandwich plate.

2.4.1 Optimization design of energy absorption

The fiber layer thickness of the CFRP upper panel, the Octet rod diameter, and the fiber layer thickness of the CFRP lower panel are taken as the structural variables for design, and the optimization design is carried out based on the DOE and surrogate optimization software LS-OPT. The DOE method of LHS is used to obtain the surrogate optimization models of the above parameters and dynamic response under 15 working conditions, as shown in Table 6.

The response surface model is established by the regression analysis, and the energy optimization design of the CFRP-lattice aluminum sandwich plate is carried out. Firstly, the fiber layer thickness of the upper panel t_1, the Octet rod diameter t_2, and the fiber layer thickness of the lower panel t_3 are taken as design variables, and the *SEA* of the structure is taken as the optimization objective. Under the constraint conditions of the above design variables and the constant mass of the CFRP-lattice aluminum sandwich plate, the maximum value of *SEA* is calculated. The constraints of the *SEA* optimization problem are as follows.

$$\begin{cases} 0.1 \leqslant t_1 \leqslant 1.4 \\ 1.4 \leqslant t_2 \leqslant 1.6 \\ 0.1 \leqslant t_3 \leqslant 1.4 \\ 1.111\,67t_1 + 0.057\,4t_2^2 + \\ \quad 1.111\,67t_3 = 0.610\,79 \end{cases} \tag{13}$$

By using the Design-Expert software, the second-order polynomial is used to fit the simulation data points and the fitting formula is as follows. The partial approximate response surface is shown in Fig. 12.

Table 6 Experimental design surrogate optimization model and its simulation results

Working condition	Fiber layer thickness of upper panel t_1/mm	Rod diameter of Octet lattice t_2/mm	Fiber layer thickness of lower panel t_3/mm	Energy/J	Mass/kg	*SEA*/(J·kg^{-1})	*Deflection*/mm
1	0.250	1.000	0.250	107.211	8.892	12.057	5.499
2	0.366	1.312	0.386	210.062	9.212	22.803	5.352
3	0.106	0.873	0.313	74.100	8.789	8.431	5.391
4	0.141	1.441	0.150	216.952	8.719	24.883	7.522
5	0.144	0.782	0.103	51.873	8.590	6.039	6.443
6	0.289	0.981	0.367	108.320	9.064	11.951	4.872
7	0.348	0.526	0.189	37.265	8.894	4.190	4.679
8	0.398	1.393	0.220	291.282	9.075	32.097	6.580
9	0.304	1.096	0.122	168.305	8.821	19.080	7.027
10	0.325	1.058	0.280	165.571	9.016	18.365	5.361
11	0.185	1.560	0.263	386.789	8.913	43.397	6.406
12	0.239	0.484	0.350	26.754	8.949	2.989	4.351
13	0.267	0.640	0.178	44.872	8.799	5.100	5.189
14	0.192	1.233	0.233	221.490	8.837	25.063	6.165
15	0.215	0.726	0.334	30.697	8.921	3.441	4.794

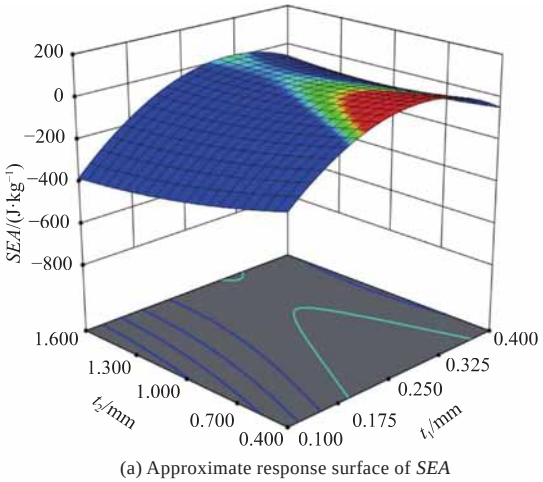

(a) Approximate response surface of *SEA*

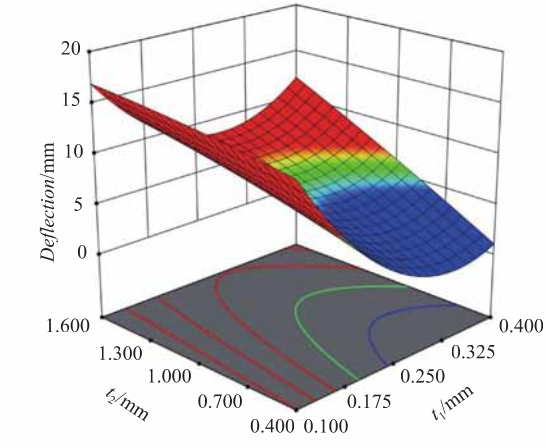

(b) Approximate response surface of lower panel deflection

Fig. 12 Response surface

$$SEA = f_1(t_1,t_2,t_3) = 3.869\,3 + 116.473t_1 - 50.861\,5t_2 + 36.188\,6t_3 + 44.543\,9t_1t_2 - 241.973t_1t_3 + 51.710\,3t_2t_3 - 199.92t_1^2 + 31.175\,2t_2^2 - 65.601\,1t_3^2 \quad (14)$$

$$Deflection = f_2(t_1,t_2,t_3) = 5.686\,03 - 4.501\,32t_1 + 3.442\,44t_2 - 10.928t_3 + 2.152\,6t_1t_2 - 7.083\,01t_1t_3 - 5.985\,83t_2t_3 + 5.699\,96t_1^2 - 0.251\,382t_2^2 + 24.307t_3^2 \quad (15)$$

The Mathematica software is used to solve the maximum *SEA* under constraint conditions, and the corresponding optimal design points (0.317, 1.6, and 0.1) are obtained. The predicted optimal *SEA* and *Deflection* are 45.300 J/kg and 8.757 mm, respectively, as shown in Table 7. Then, the verification analysis is carried out at the optimal design points, and the *SEA* and *Deflection* of the optimal design are 46.287 J/kg and 8.327 mm, with errors of 2.18% and 4.91%, respectively. The optimization results show that when the thickness of the lower panel is the smallest, and the Octet rod diameter is the largest, *SEA* reaches the peak. The *SEA* value of the optimization design is 284% higher than that of the uniform design. However, it can also be seen that the deflection of the lower panel is 51.4% higher than that in the original design.

Table 7 Optimization design and simulation results of energy absorption

Parameter	Optimization result	Simulation result
Energy/J	–	411.272
Mass/kg	–	8.885
SEA/(J·kg^{-1})	45.300	46.287
Deflection/mm	8.757	8.327

2.4.2 Optimization design of energy absorption and deformation

The results of the above energy absorption optimization design show that a decrease in the thickness of the lower panel can help to improve the energy absorption efficiency of the sandwich plate structure. In terms of the local protection of ships, the paper should not only focus on the energy absorption problem but also on the large deformation and deflection of the plate. Therefore, this section will analyze the optimization problem of the deformation of the lower panel based on the above section. Here, *SEA* is still taken as the optimization objective. Under the premise that the mass of the sandwich plate structure is constant, the deflection constraint of the lower panel is added to make it less than 5.499 mm set in the original design. In this case, the constraints of the *SEA* optimization problem are as follows.

$$\begin{cases} 0.1 \leqslant t_1 \leqslant 1.4 \\ 1.4 \leqslant t_2 \leqslant 1.6 \\ 0.1 \leqslant t_3 \leqslant 1.4 \\ 5.686\,03 - 4.501\,32t_1 + 3.442\,44t_2 - \\ \quad 10.928t_3 + 2.152\,6t_1t_2 - 7.083\,01t_1t_3 - \\ \quad 5.985\,83t_2t_3 + 5.699\,96t_1^2 - 0.251\,382t_2^2 + \\ \quad 24.307t_3^2 \leqslant 5.499 \\ 1.111\,67t_1 + 0.057\,4t_2^2 + 1.111\,67t_3 = 0.610\,79 \end{cases} \tag{16}$$

The obtained corresponding optimal design points are 0.161, 1.115, and 0.324, and the predicted optimal *SEA* and *Deflection* are 18.367 J/kg and 5.499 mm, respectively, as shown in Table 8. Then, the verification analysis is carried out at the optimal design points, and the *SEA* and *Deflection* of the optimal design are 19.151 J/kg and 5.467 mm, with errors of 4.27% and −0.58%, respectively.

Table 8 Optimization design and simulation results of energy absorption and deformation

Parameter	Optimization result	Simulation result
Energy/J	–	170.233
Mass/kg	–	8.889
SEA/(J·kg^{-1})	18.367	19.151
Deflection/mm	5.499	5.467

Fig. 13 compares the two optimization simulation results with the results under working condition A. It can be seen that the energy absorption performance of the structure has been greatly improved under the first optimization method. Under the second optimization method, the energy absorption performance of the structure is also improved by 59% when the deformation of the lower panel is not excessive.

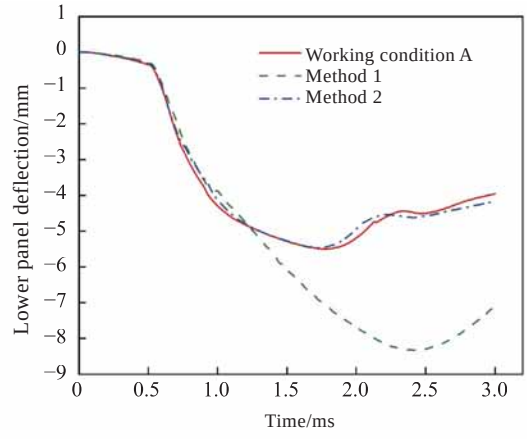

(a) Deflection-time curves of lwer panel

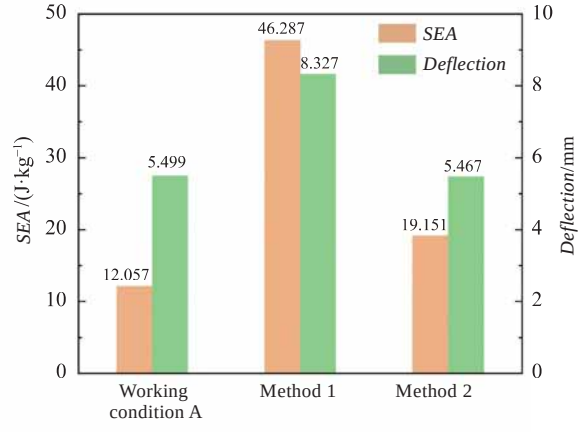

(b) *SEA* and *Deflection*

Fig. 13 Optimization simulation results

3 Conclusions

In order to study the protective effect of the sandwich plate structure on the local deformation and damage of ships under the noncontact underwater explosion shock wave load, the numerical simulation method is used to explore the characteristics of the nonexplosive and noncontact underwater explosion shock wave load. Firstly, the dynamic response characteristics and the overall dynamic large plastic deformation process of the CFRP-lattice aluminum sandwich plate under the noncontact underwater explosion shock wave load are studied. Then, the surrogate optimization model of structural design parameters and deformation response is obtained by

the DOE method, and the correlation between different parameters and the objective function is analyzed. Finally, the optimal design scheme is obtained by solving the optimization problem based on the protection requirements and constraints. The main conclusions are as follows.

1) In this paper, the numerical simulation method is used to explore the characteristics of the equivalent nonexplosive and noncontact underwater explosion shock wave load. The comparison with the experimental results in the existing literature shows that the method is in good agreement with these results, which can provide a reliable method for studying the anti-shock performance of the local structure of the ship.

2) Three structural design parameters, i. e., the fiber layer thickness of the upper panel, the Octet rod diameter, and the fiber layer thickness of the lower panel are selected to explore their influence on the energy absorption performance of the CFRP-lattice aluminum sandwich plate. It is found that compared with the non-gradient structure, the gradient structure can better absorb energy, and as the rod diameter of the lattice structure increases, the energy absorption performance of the structure will be enhanced greatly.

3) RSM is used to optimize the energy absorption of the CFRP-lattice aluminum sandwich plate. Under constant plate mass, surrogate optimization models are established by selecting appropriate parameters mentioned above to solve the problem, and an optimal design on the thickness of the upper panel, the Octet rod diameter, and the thickness of the lower panel is obtained. The reliability of the optimization results is verified by the comparison with the numerical simulation results. The research shows that optimal sizes of the three design parameters can be obtained by increasing the thickness of the upper panel, reducing the thickness of the lower panel, and improving the diameter of the lattice material, so as to realize an optimal anti-shock performance of the structure.

References

[1] ZHANG A M, WANG S P, WANG Y, et al. Advances in the research of characteristics of warship structural damage due to underwater explosion [J]. Chinese Journal of Ship Research, 2011, 6 (3): 1−7 (in Chinese).

[2] XIN C L, QIN J, XU G G, et al. Application of numerical simulation software in underwater explosion simulation [C]//The 4th National Conference on Experimental Technology of Explosion Mechanics. Mount Wuyi: Chinese Society of Mechanics, 2006 (in Chinese).

[3] JIAO A L, JIA Z, CHEN G J. The research of shock response on warship subjected to a close underwater explosion based on ABAQUS [J]. Electronic Design Engineering, 2015, 23 (10): 179−181, 185 (in Chinese).

[4] COLE P. Underwater explosion[M]. LUO Y J, HAN RZ, GUAN X, et al, trans. Beijing: National Defense Industry Press, 1960 (in Chinese).

[5] GEERS T L. Doubly asymptotic approximations for transient motions of submerged structures [J]. Journal of the Acoustical Society of America, 1978, 64 (5): 1500−1508.

[6] LI G H, LI Y J, ZHANG X C, et al. Shock spectrum measurement and analysis of underwater explosion on a floating shock platform [J]. Journal of Ship Mechanics, 2000, 4 (2): 51−60 (in Chinese).

[7] BERNAL OSTOS J, RINALDI R G, HAMMETTER CM, et al. Deformation stabilization of lattice structures via foam addition [J]. Acta Materialia, 2012, 60 (19): 6476−6485.

[8] YAO X L, HOU J, WANG Y H, et al. Research on simulation of underwater shock environment of ship [J]. Shipbuilding of China, 2003, 44 (1): 71−74 (in Chinese).

[9] YU J, LIU G Z, WANG J, et al. An effective method for modeling the load of bubble jet in underwater explosion near the wall [J]. Ocean Engineering, 2021, 220: 108408.

[10] JIANG X W, ZHANG W, LI D C, et al. Experimental analysis on dynamic response of pre-cracked aluminum plate subjected to underwater explosion shock loadings [J]. Thin-Walled Structures, 2021, 159: 107256.

[11] WANG X H, ZHANG S R, WANG C, et al. Blast-induced damage and evaluation method of concrete gravity dam subjected to near-field underwater explosion [J]. Engineering Structures, 2020, 209: 109996.

[12] YAO X L, WANG Y H, SHI D Y, et al. Numerical experiment on underwater explosion of cylinder [J]. Journal of Harbin Engineering University, 2002, 23 (1): 5−8, 36 (in Chinese).

[13] HUANG C, LIU M B, WANG B, et al. Underwater explosion of slender explosives: directional effects of shock waves and structure responses [J]. International Journal of Impact Engineering, 2019, 130: 266−280.

[14] HAN Y. A numerical simulation of explosion loads and bull response [D]. Wuhan: Huazhong University of Science&Technology, 2019 (in Chinese).

[15] HUANG Z X, ZHANG X, YANG C Y. Experimental and numerical studies on the bending collapse of multi-cell aluminum/CFRP hybrid tubes [J]. Composites Part B: Engineering, 2020, 181: 107527.

[16] AI D J. Research on failure mechanism and energy absorption characteristics of sandwich panels with aluminum foam core under contact and non-contact near-field water blast loading [D]. Wuhan: Huazhong University of Science & Technology, 2017 (in Chinese).

[17] ELSAYYED M S A, DAMIANO P. Multiscale model of the effective properties of the octet-truss lattice material [C]//USA: Aiaa/issmo Multidisciplinary Analysis and Optimization Conference, 2008: 847−850.

[18] USHIJIMA K, CANTWELL W J, MINES R A W, et al. An investigation into the compressive properties of stainless steel micro-lattice structures [J]. Journal of Sandwich Structures&Materials, 2011,13(3): 303−329.

[19] DENARDO N, PINTO M, SHUKLA A. Hydrostatic and shock-initiated instabilities in double-hull composite cylinders [J]. Journal of the Mechanics and Physics of Solids, 2018, 120: 96−116.

[20] ZHANG X, ZHANG H, WANG Z. Bending collapse of square tubes with variable thickness [J]. International Journal of Mechanical Sciences, 2016, 106: 107−116.

[21] ZHANG X. Crashworthiness analysis and design optimization of light thin-walled structures [D]. Dalian: Dalian University of Technology, 2007 (in Chinese).

[22] ZHANG Z H, HE Z, GUO W. A comparative study of three central composite designs in response surface methodology [J]. Journal of Shenyang Institute of Aeronautical Engineering, 2007, 24 (1): 87−91 (in Chinese).

[23] MCKAY M D, BECKMAN R J, CONOVER W J. Comparison of three methods for selecting values of input variables in the analysis of output from a computer code [J]. Technometrics, 1979, 21 (2): 239−245.

[24] DESHPANDE V S, HEAVER A, FLECK N A. An underwater shock simulator [J]. Proceedings of the Royal Society A: Mathematical, Physical and Engineering Sciences, 2006, 462 (2067): 1021−1041.

[25] REN P. Research on non-explosive underwater shock loading technique and blast resistant properties of aluminium alloy structures [D]. Wuhan: Huazhong University of Science & Technology, 2017 (in Chinese).

[26] LI Y, CHEN Z H, ZHAO T, et al. An experimental study on dynamic response of polyurea coated metal plates under intense underwater impulsive loading [J]. International Journal of Impact Engineering, 2019, 133: 103361.

[27] HUANG W, JIA B, ZHANG W, et al. Dynamic failure of clamped metallic circular plates subjected to underwater impulsive loads [J]. International Journal of Impact Engineering, 2016, 94: 96−108.

[28] ZHU L X, WANG T Y, ZHU L X. Optimization design of a functionally graded lattice sandwich structure based on gradient factor [J]. Journal of Vibration and Shock, 2018, 37 (23): 98−103, 110 (in Chinese).

水下爆炸载荷下复合点阵夹层结构冲击响应分析

毛柳伟[1], 祝心明[2], 黄治新[3], 李营[*3]

1 海军研究院, 北京 100161

2 武汉理工大学 理学院, 武汉 430063

3 北京理工大学 先进结构技术研究院, 北京 100081

摘　要: [**目的**] 为提升舰船的水下抗爆能力, 针对水下爆炸冲击波作用下新型防护结构碳纤维增强复合材料(CFRP)−点阵铝夹芯板的抗冲击能量吸收性能展开研究。[**方法**] 首先, 利用有限元软件 ABAQUS 建立非药式非接触水下爆炸载荷下 CFRP−点阵铝夹芯板的数值仿真模型, 并验证其可靠性; 然后, 通过控制单一变量来分析 CFRP−点阵铝夹芯板上、下面板每层纤维厚度和点阵夹芯结构杆件直径对其能量吸收性能与结构挠度的影响; 最后, 基于上述 3 种设计参数, 采用实验设计方法和数值模拟方法建立代理优化模型, 用于对 CFRP−点阵铝夹芯板结构的能量吸收性能进行优化设计。[**结果**] 结果显示: 在 CFRP−点阵铝夹芯板质量恒定的情况下, 其优化结果可使比吸收能提高 284%; 在充分考虑下面板变形的情况下, 优化结果的比吸收能可提高 59%。[**结论**] 研究表明, 该 CFRP−点阵铝夹芯板优化结构可有效提升其能量吸收性能, 而响应面法是一种可有效提高结构能量吸收性能的优化方法。

关键词: 水下爆炸; 点阵结构; 优化设计; 数值模拟